Published in final edited form as:
Biopolymers. 2009 August ; 91(8): 633–641. doi:10.1002/bip.21192.

Solution Structure of A Novel T-cell Adhesion Inhibitor Derived from the Fragment of ICAM-1 Receptor: Cyclo(1,8)-Cys-Pro-Arg-Gly-Gly-Ser-Val-Cys

Bimo A. Tejo[1] and **Teruna J. Siahaan**[*]
Department of Pharmaceutical Chemistry, The University of Kansas, 2095 Constant Avenue, Lawrence, KS 66047

Abstract

This study is aimed at elucidating the structure of a novel T-cell adhesion inhibitor, cyclo(1,8)-CPRGGSVC using one- and two-dimensional ^{1}H NMR and molecular dynamics (MD) simulation. The peptide is derived from the sequence of its parent peptide cIBR (cyclo(1,12)-PenPRGGSVLVTGC), which is a fragment of intercellular adhesion molecule-1 (ICAM-1). Our previous results show that the cyclo(1,8)-CPRGGSVC peptide binds to the LFA-1 I-domain and inhibits heterotypic T-cell adhesion, presumably by blocking the LFA-1/ICAM-1 interactions. The structure of the peptide was determined using NMR and MD simulation in aqueous solution. Our results indicate that the peptide adopts type-I β-turn conformation at the Pro2-Arg3-Gly4-Gly5 (PRGG) sequence. The β-turn structure at the PRGG motif is well conserved in cIBR peptide and ICAM-1 receptor, which suggests the importance of the PRGG motif for the biological activity of cyclo(1,8)-CPRGGSVC peptide. Meanwhile, the Gly5-Ser6-Val7-Cys8-Cys1 (GSVCC) sequence forms a “turn-like” random coil structure that does not belong to any structured motif. Therefore, cyclo(1,8)-CPRGGSVC peptide has only one structured region at the PRGG sequence, which may play an important role in the binding of the peptide to the LFA-1 I-domain. The conserved β-turn conformation of the PRGG motif in ICAM-1, cIBR, and cyclo(1,8)-CPRGGSVC peptides can potentially be used to design peptidomimetics.

Keywords

autoimmune diseases; β-turn; ICAM-1; LFA-1; T-cell adhesion

INTRODUCTION

Human immune response is activated when thymus-derived lymphocyte (T cell) contacts an antigen-presenting cell (APC) by forming an immunological synapse.[1–3] This contact zone consists of two signals: a primary signal (Signal-1) that comes from the interaction between the T-cell receptor (TCR) and antigen-MHC-II complex, and a co-stimulatory signal (Signal-2) that originates from the attachment of several molecules such as leukocyte function-associated antigen-1 (LFA-1) and the intercellular adhesion molecule-1 (ICAM-1).[4–6] The formation of an immunological synapse followed by the immune response is required by the human body as part of its defense mechanism. However, in autoimmune diseases, it could harm the host body if the T cell recognizes the host's tissue as an antigen.

[*]*Corresponding Author:* Dr. Teruna J. Siahaan Department of Pharmaceutical Chemistry, The University of Kansas, Simons Research Laboratories, 2095 Constant Avenue, Lawrence, KS 66047, USA. Tel.: (785) 864-7327 Fax: (785) 864-5736 siahaan@ku.edu.
[1]Current address: Department of Chemistry, Faculty of Science, Universiti Putra Malaysia, 43400 UPM Serdang, Malaysia

Therefore, blocking of formation of the immunological synapse could be significant in suppressing autoimmune diseases and allograft rejection.

Choosing the right target molecule to block an immune synapse requires a depth of knowledge of molecular actions during synapse formation. It has been proposed that during early events of immune synapse formation LFA-1/ICAM-1 complex (Signal-2) is formed at the center of the T-cell/APC interface. The LFA/ICAM-1 complex forces the outermost ring of the T-cell membrane to move closer to the APC to enable the formation of TCR-Ag-MHC complex (Signal-1). This event is followed by translocation of Signal-1 to the center of the synapse and Signal-2 to the edge of the T-cell/APC interface.3 The mechanism of immune synapse formation suggests that blocking the LFA-1/ICAM-1 interactions (Signal-2) could influence the formation of TCR-Ag-MHC complex (Signal-1), thus playing a significant role in suppressing the autoimmune response.7 In addition to altering the formation of the immune synapse, blocking of LFA-1/ICAM-1 interactions has also been shown to alter the immune response via induction of a certain T-cell phenotype (*i.e.*, Th-1 or Th-2).8

Inhibition of ICAM-1/LFA-1 interactions with monoclonal antibodies to ICAM-1 and LFA-1 has been shown to suppress allograft rejection9،10 and autoimmune diseases such as psoriasis,11،12 type-1 diabetes,13 and rheumatoid arthritis.14،15 Besides antibodies, several small molecules,16،17 peptides,18،19 and peptidomimetics20 have been developed as inhibitors for LFA-1/ICAM-1 interactions. Our group has discovered several LFA-1/ICAM-1 peptide inhibitors derived from the sequences of LFA-1 and ICAM-1.19 One of the peptides, called cIBR (cyclo(1,12)-PenPRGGSVLVTGC), has been shown to inhibit homotypic and heterotypic adhesion of T cells.21،22 This peptide has also been shown to bind to the I-domain of LFA-1 receptor on MIDAS and L-site.23،24

The solution structure of cIBR peptide showed that the Pro2-Arg3-Gly4-Gly5 (PRGG) region forms a β-turn structure that mimics the conformation of the same region on its parent ICAM-1 molecule.25 It has been shown that turn motifs are usually present on the surface of proteins and are likely involved in the protein-protein interactions.26 Our initial results indicated that the PRGG motif in cIBR peptide is important for the biological activity of the peptide.22 Then, we synthesized several fragments of cIBR peptide by reducing the size of the peptide from the C-terminus. We found that the shorter derivative of cIBR peptide, namely, cyclo(1,8)-CPRGGSVC peptide, showed better activity than other cIBR derivatives, even slightly better than its parent cIBR peptide.27 The smaller size of cyclo(1,8)-CPRGGSVC and its lower hydrophobicity than its parent peptide (cIBR) potentially enable this peptide to be conjugated to hydrophobic drugs for targeted drug delivery without creating highly hydrophobic conjugates as happened to cIBR-Dox.28 The smaller size of cyclo(1,8)-CPRGGSVC also makes this peptide a good candidate for designing peptidomimetics.

In this work, we determined the conformation of cyclo(1,8)-CPRGGSVC peptide using one-dimensional and two-dimensional ^{1}H NMR and molecular dynamics simulation. We found that the cyclo(1,8)-CPRGGSVC peptide retains only the β-turn conformation at the PRGG motif; however, it lacks the second β-turn structure found in cIBR peptide. This result suggests that the PRGG motif and conformation play an important role in the peptide activity in inhibiting of T-cell adhesion.

RESULTS

Residue Assignment

Two-dimensional TOCSY and ROESY spectra were used to assign each proton resonance and the proton connectivities. The fingerprint region of the TOCSY spectrum shows through-bond connectivities between amide protons and side chain protons (Figure 1a and Table 1). The amide proton of Arg3 shows through-bond connectivities to its respective HCα, HCβ, HCγ, and HCδ. The amide protons of Ser6 and Cys 8 show connectivities to their respective HCα and HCβ. Both Gly4 and Gly 5 have connectivities between their amide protons to HCα. Gly4 shows two geminal HCα, while Gly5 shows only one HCα in the TOCSY spectrum. The amide proton of Val7 has connectivities to its respective HCα, HCβ, and HCγ. The N-terminal proton of Cys1 cannot be identified due to fast exchange with water protons. Because Pro2 lacks the amide proton, this residue does not show any peak in amide proton connectivity.

The two-dimensional ROESY spectrum of the NH-HCα region was used to identify the sequential connectivities of neighboring residues (Figure 1b). The resonances for Gly4 and Gly5 were identified by their respective $d_{N\alpha}$ sequential connectivities to Arg3 and Ser6, respectively. The complete sequential “backbone walk” of all residues in the peptide, which consists of 12 ROE cross-peaks, including $d_{\alpha N}(i, i+1)$ and $d_{N\alpha}(i, i)$ ROE cross-peaks is: $d_{\alpha N}$ of Pro2-Arg3 (peak 1), $d_{N\alpha}$ of Arg3 (peak 2), $d_{\alpha N}$ of Arg3-Gly4 (peak 3), $d_{N\alpha}$ of Gly4 (peak 4), $d_{\alpha N}$ of Gly4-Gly5 (peak 5), $d_{N\alpha}$ of Gly5 (peak 6), $d_{\alpha N}$ of Gly5-Ser6 (peak 7), $d_{N\alpha}$ of Ser6 (peak 8), $d_{\alpha N}$ of Ser6-Val7 (peak 9), $d_{N\alpha}$ of Val 7 (peak 10), $d_{\alpha N}$ of Val7-Cys8 (peak 11), and $d_{N\alpha}$ of Cys8 (peak 12) (Figure 1b). Cys1-Pro2 connectivity was not observed due to fast exchange of Cys1 amide protons with water.

Chemical Shift Assignments

Because the chemical shift of HCα depends on the backbone dihedral angles (φ and ψ) and on the local chemical environment, the *chemical shift index* (CSI), which defines the difference between the measured chemical shifts and the chemical shifts when the peptide is in a statistical coil structure, can be used to elucidate the secondary structure adopted by the peptide.29 The CSI values can be negative (−1) or positive (+1), depending on whether the measured HCα chemical shift of an amino acid is lower or higher than the HCα chemical shift of the amino acid in a random-coil chemical. A peptide with a helical structure must have four or more sequential residues with negative CSI values; β-strand peptides are indicated by three or more sequential residues with positive CSI values.

In cyclo(1,8)-CPRGGSVC, no four sequential residues have negative SCI values, indicating that the peptide does not adopt a helical conformation (Figure 2). The possibility of the peptide adopting β-strand structure can also be ruled out because no three consecutive residues have positive CSI values. This suggests that the peptide adopts the turn structure or a random coil. However, the CSI values could not be used to indicate these two structures; thus, the ROE pattern and $^3J_{NH\text{-}HC\alpha}$ scalar coupling constants are needed to determine the conformation of the peptide.

ROE Pattern and $^3J_{NH\text{-}HC\alpha}$ Scalar Coupling Constants

The conformation of cyclo(1,8)-CPRGGSVC peptide was determined by evaluating the ROE connectivities (Figure 1c) and $^3J_{NH\text{-}HC\alpha}$ scalar coupling constant (Figure 3 and Table 2). The possibility of the peptide adopting helical structure could be ruled out because there were no characteristic ROE cross-peaks from $d_{NN}(i, i+1)$, $d_{\alpha N}(i, i+3)$, $d_{\alpha N}(i, i+4)$, and $d_{\alpha\beta}(i, i+3)$. In addition, there were no characteristic ROE cross-peaks for β-strand structure, which are strong $d_{\alpha N}(i, i+1)$ cross-peaks but without $d_{NN}(i, i+1)$. The presence of $d_{NN}(i, i+1)$ and

$d_{\alpha N}(i, i+1)$ ROE cross-peaks indicates the propensity to adopt a *turn structure*. Four $d_{NN}(i, i+1)$ ROE cross peaks were found, *i.e.* Arg3-Gly4, Gly4-Gly5, Ser6-Val7, and Val7-Cys8 (Figure 1c). The $d_{NN}(i, i+1)$ ROE cross-peak of Gly5-Ser6 was too weak to observe. This suggests that the peptide has two turns. The first is a type-I β-turn at Pro2-Arg3-Gly4-Gly5 (PRGG), which is supported by the successive $d_{NN}(i, i+1)$ ROE cross-peaks of Arg3-Gly4 and Gly4-Gly5. The dihedral angle (φ) calculated from $^3J_{NH\text{-}HC\alpha}$ coupling constants (Table 2) confirms that the PRGG sequence has the propensity to form a type-I β-turn. The calculated φ of Arg3 (i+1) and Gly4 (i+2) fall within the 30° deviation limit from the ideal φ for type-I β-turn conformation;26 Arg3 has a calculated φ of −79.46° (ideal φ for type-1 β-turn is −60°) and Gly4 has a calculated φ of −70.28° compared to the ideal φ of −90°. The small values of $^3J_{NH\text{-}HC\alpha}$ of Arg3 (6.65 Hz), Gly4 (5.48 Hz), and Gly5 (5.67 Hz) also suggest that the PRGG sequence adopts turn structure (Table 2).

Since we identified Pro2-Arg3-Gly4-Gly5 adopts a type-I β-turn structure, we expected to see a $d_{\alpha N}(i, i+2)$ ROE cross-peak between Arg3 and Gly5. However, our observation shows that this $d_{\alpha N}(i,i+2)$ ROE cross-peak is very weak. Our effort to lower the contour level results in a very complex ROESY spectrum that might cause difficulties for the readers to see the important $d_{N\alpha}(i, i)$ and $d_{\alpha N}(i, i+1)$ cross-peaks for the sequential "backbone walk" (Fig. 1b).

The second turn is observed at the Gly5-Ser6-Val7-Cys8 (GSVC) sequence, and the determination of its turn type is not as straightforward and conclusive as in the PRGG sequence. The presence of successive $d_{NN}(i, i+1)$ ROE cross-peaks of Ser6-Val7 and Val7-Cys8 suggests that the GSVC sequence may adopt a type-I β-turn as in the PRGG sequence. The Ser6 (i+1) has a calculated φ of −89.25° that deviates less than 30° from the ideal φ of −60°, while Val7 has a calculated φ of −96.98°, close to the ideal value of −90° (Table 1). The $^3J_{NH\text{-}HC\alpha}$ values for GSVC are larger than the values in the PRGG sequence. Only one residue (Gly5) has $^3J_{NH\text{-}HC\alpha}$ value less than 6.0 Hz, while Ser6 has $^3J_{NH\text{-}HC\alpha}$ value of 7.83 Hz and Val7 has $^3J_{NH\text{-}HC\alpha}$ values larger than 8 Hz (Table 2), suggesting that the GSVC sequence may not have a classical β-turn structure. Because the determination of GSVC secondary structure using ROE patterns and $^3J_{NH\text{-}HC\alpha}$ scalar coupling constant did not give a conclusive result, molecular dynamics simulation of the peptide using ROE restraint was performed to help elucidate the conformation of the GSVC sequence.

Molecular Model of the Peptide Structure

The three-dimensional structure of the peptide was determined by restrained molecular dynamics (MD) simulation using ROE distance restraints and peptide bond (ω) dihedral angle restraint of 180 ± 10° to keep all peptide bond as *trans*, except for Cys1-Pro2 peptide bond. From the last 500 ps of MD trajectories, all interproton distances are deviated less than 0.5 Å from the upper boundaries of ROE distance restraints (Table 3). The MD-simulated φ angles for all residues in the peptide are within 30° of the φ values calculated from the $^3J_{NH\text{-}HC\alpha}$, except Gly5 that has one φ value outside the 30° deviation limit, presumably due to the flexibility of this residue (Table 2). Ten structures from the MD simulation were taken as an ensemble of the peptide structures in solution (Figure 4a).

The presence of a type-I β-turn at the PRGG sequence was confirmed by the φ and ψ angles from the last 500 ps trajectories of the MD simulation. The average φ and ψ angles of residues at the PRGG sequence are (φ°, ψ°): Pro2 (−78.0 ± 8.2°, 163.2 ± 6.3°), Arg3 (−88.6 ± 7.0°, −24.8 ± 11.25°), Gly4 (−72.1 ± 12.1°, 15.2 ± 13.8°). Gly5 has two sets of φ angles (−169.6 ± 19.3° and 171.7 ± 6.3°) and ψ angles (−174.7 ± 4.3° and 167.4 ± 8.1°) (Table 2), which are due to the flexibility of the Gly5 backbone. The simulated and *J*-coupling calculated φ and ψ angles of residues Arg3 (i+1) and Gly4 (i+2) are less than 30° from the ideal angles for the type-I β-turn structure.26 Another indicator of β-turn structure is that the

distance from the Cα atom at residue *i* to the Cα atom at residue *i*+3 must be 7 Å or less.26 The Cα-Cα distance between Pro2 (*i*) and Gly5 (*i*+3) is 6.9 ± 0.2 Å, which confirms the presence of a β-turn at the PRGG sequence (Figure 4b). The turn structure of the PRGG sequence is stabilized by a hydrogen bond between the backbone carbonyl group of Pro2 and the amide proton of Gly 5 (3.1 ± 0.3 Å) (Figure 4b), which suggests that the PRGG motif in this peptide has a closed type-I β-turn conformation. The involvement of the Gly5 amide proton in hydrogen bonding is also indicated by the small value of the Gly5 temperature coefficient (−3.9 ppb/K) (Figure 5).

The MD simulation result did not confirm the presence of a type-I β-turn structure at the GSVC sequence. The simulated (φ°, ψ°) angles of Ser6 (*i*+1) and Val7 (*i*+2) were (−148.2 ± 6.9°, 99.7 ± 6.4°) and (−144.6 ± 8.5°, −56.5 ± 7.0°), respectively. These values fall outside the 30° deviation limit from the ideal values of φ and ψ angles of (*i*+1) and (*i*+2) residues for the type-I β-turn structure.26 Visual observation of the ensemble of 10 structures from the last 500 ps trajectories of the MD simulation showed no β-turn structure on the GSVC sequence. However, a “turn-like” structure could be found at GSVCC sequence (Figure 4). This turn-like structure involves five residues and is stabilized by a hydrogen bond between the backbone carbonyl of Gly5 and the amide proton of Cys1 with a distance of 2.2 ± 0.3 Å. Meanwhile, the Cα-Cα distance between Gly5 and Cys1 is 6.4 ± 0.4 Å, which is close to the ideal Cα-Cα distance for type-I (6.31 Å) and type-II (6.26 Å) α-turns.30 Since the GSVCC sequence is stabilized by a hydrogen bond and the Cα-Cα distance between Gly5 and Cys1 falls within the ideal Cα-Cα distance for a type-I or type-II α-turn structure, one might think that the GSVCC sequence adopts these two types of α-turn structure. However, simulated φ and ψ angles of GSVCC residues fall outside the 30° deviation limit from the ideal φ and ψ angles for type-I or type-II α-turn structure.30 The high $^{3}J_{\mathrm{NH\text{-}HC\alpha}}$ coupling constant values of Ser6 and Val7 suggests that the “turn-like” structure at GSVCC residues does not belong to the α-turn structure. It is possible that the “turn-like” structure around residues Gly5-Ser6-Val7-Cys8-Cys1 was randomly formed due to the side-chain cyclization between Cys1 and Cys8. Therefore, the cyclo(1,8)-CPRGGSVC has adopted the type-I β-turn conformation at the PRGG sequence and a “turn-like” structure at the GSVCC sequence.

Hydrogen Bonding Analysis of Amide Protons

In peptides, the amide proton chemical shifts are sensitive to temperature changes. The amide protons involved in intramolecular hydrogen bonding are less sensitive to temperature changes than amide protons that are solvent-accessed and not involved in intramolecular hydrogen bonding network. The involvement of amide protons in hydrogen bonding can be measured by calculating the temperature coefficient (Δδ/ΔT), which is the slope of amide proton chemical shift changes over different temperatures.31 Small values of Δδ/ΔT (−3 ppb/K or less) indicate amide protons that are involved in intramolecular hydrogen bonding and less exposed to the solvent. On the other hand, high values of Δδ/ΔT (−5 ppb/K or more) suggest amide protons that are more exposed to the solvent.32

Our result indicates that Gly4 and Gly5 may have more involvement in intramolecular hydrogen bonding than the other residues (Figure 5). The Δδ/ΔT values of Gly4 and Gly5 are −3.6 ppb/K and −3.9 ppb/K, respectively. The Δδ/ΔT values of the other residues are (ppb/K): −14.0 (Arg3), −8.3 (Ser6), −6.7 (Val7), and −8.7 (Cys8). This suggests that there are two possible intermolecular hydrogen bonds that involve the amide protons of Gly4 and Gly5. The backbone carbonyl groups that might form hydrogen bonds with Gly4 or Gly5 can be determined by observing the three-dimensional structure of the peptide determined by ROE-restraint molecular dynamics simulation.

Interestingly, the three-dimensional structure of the peptide shows two intramolecular hydrogen bonds between the backbone carbonyl group of Pro2 and the amide protons of

Gly4 and Gly5 (Figure 4b). The first hydrogen bond between Pro2 and Gly5 is responsible for the stability of the β-turn of the PRGG motif as mentioned before. The second hydrogen bond between Pro2 and Gly4 (Pro2 CO – Gly4 NH = 2.9 ± 0.4 Å) is suggested to strengthen the rigidity of the β-turn conformation at the PRGG sequence.

DISCUSSION

We have shown that cyclo-CPRGGSVC is a good inhibitor of heterotypic T-cell adhesion.27 The unique type-I β-structure at the PRGG sequence and a “turn-like” random coil structure at the GSVCC sequence may contribute to its biological activity. This peptide is the result of a reduction in the size of cIBR (cyclo(1,12)-PenPRGGSVLVTGC) peptide to pinpoint the essential residues that play an active role in the biological activity of the cIBR peptide.27 Cyclo(1,8)-CPRGGSVC was found to have slightly better activity than the parent cIBR peptide in inhibiting heterotypic T-cell adhesion.27 This supports our previous hypothesis that the PRGG motif is vital for the function of both cyclo(1,8)-CPRGGSVC and cIBR peptide.22،25 It is interesting to find that the PRGG motif in cyclo(1,8)-CPRGGSVC peptide maintains the type-I β-turn structure similar to that in the parent cIBR peptide. The cIBR peptide has three consecutive turns: a type-I or type-II β-turn at Pro2-Arg3-Gly4-Gly5, a type-I β-turn at Gly5-Ser6-Val7-Leu8, and a type-I β-turn at Val9-Thr10-Gly11-Cys12.25 It is noteworthy to mention that the β-turn structure of the PRGG motif in cyclo(1,8)-CPRGGSVC and cIBR peptides, both of whose sequences were derived from the parent molecule ICAM-1 receptor, is structurally similar to the β-turn structure of the Pro12-Arg13-Gly14-Gly15 region of ICAM-1.25

Why is the PRGG motif so important? We have shown that the cIBR peptide binds to the MIDAS (metal-ion dependent adhesion site) and L-site (allosteric site) of the LFA-1 I-domain.23،24 The crystal structure of LFA-1/ICAM-1 complex shows that MIDAS is located at the interface between two receptors;33 therefore, the binding of cIBR to MIDAS may directly disrupt the LFA-1/ICAM-1 interaction. However, the mechanism of inhibition of T-cell adhesion by cIBR that binds to L-site is not straightforward. We have shown that the cIBR peptide binds to the L-site by extending the Gly5 to Gly11 residues to the hydrophobic pocket of the L-site, while the Arg3 side chain of cIBR hinders the movement of the α7 helix of the LFA-1 I-domain.27 Molecular dynamics simulation of LFA-1 complexed with lovastatin suggests that the binding of small molecules to the hydrophobic pocket of the L-site greatly reduces the free movement of α7 helix that is vital for LFA-1 functions;34 therefore, inhibition of this movement may enable the LFA-1 receptor to bind to ICAM-1 receptor. Meanwhile, the results of our initial fluorescence binding study results suggest that the cyclo(1,8)-CPRGGSVC peptide also binds to the LFA-1 I-domain (data not shown). The computational docking study shows an interesting feature of how the cyclo(1,8)-CPRGGSVC peptide can inhibit the interaction of LFA-1 to ICAM-1. The Arg3 side chain interacts with the Lys305 residue that is located at the α7 helix of the LFA-1 I-domain.27 These results suggest that Arg3 in cIBR and cyclo(1,8)-CPRGGSVC peptides plays an important role in inhibiting the binding of LFA-1 to ICAM-1 by reducing the motion of the α7 helix region.

In conclusion, we have shown that the cyclo(1,8)-CPRGGSVC peptide maintains the β-turn conformation at the PRGG motif similar to its parent peptide, cIBR. Reducing the size of a twelve-residue-long cIBR peptide to the eight-residue-long cyclo(1,8)-CPRGGSVC peptide does not compromise the biological activity or the structure of the PRGG motif of the peptide. With smaller size and less hydrophobicity, cyclo(1,8)-CPRGGSVC peptide is a good candidate to be conjugated to drug compounds and can be used in targeted drug delivery. The structurally well-conserved PRGG motif may be used in a peptidomimetic approach to search for a better LFA-1/ICAM-1 inhibitor.

MATERIALS AND METHODS

Peptide Synthesis

Cyclo(1,8)-CPRGGSVC was synthesized by standard Fmoc solid phase peptide chemistry on Fmoc-L-Cys(Trt)-PAL-PEG-PS resin (Applied Biosystems, Foster City, CA) using the automated peptide synthesizer (PerSeptive Biosystems, Framingham, MA). All couplings were carried out in DMF using HATU/DIEA as activator and 20% piperidine as deblocking solution. Upon completion of the synthesis, the peptide was cleaved from the resin using a cleavage mixture (reagent B) consisting of 95% trifluroacetic acid (TFA), 0.5% thioanisole, 0.3% ethanedithiol, and 0.2% anisole for 2 h at room temperature under nitrogen blanket. Then, the mixture of resin and reagent B was filtered and the filtrate was added into cold ether to yield a white precipitate of the crude peptide. The peptide was purified using semi-preparative HPLC on a C-18 reverse phase column (Varian, Palo Alto, CA). Cyclization of the pure linear peptide was accomplished by air oxidation in ammonium bicarbonate buffer (0.05 M, pH 8.5) overnight in high dilution (0.06 mM). After cyclization, the peptide solution was concentrated using a rotary evaporator to 10 mL followed by lyophilization. The lyophilized powder containing peptide (10%) and ammonium bicarbonate (90%) was then purified on semi-preparative HPLC using a C-18 column. The pure fractions of the peptide were pooled and lyophilized. The molecular weight of the peptide was determined by MALDI-TOF mass spectrometry.

NMR Spectroscopy

Two-dimensional NMR experiments were carried out on a Bruker Avance spectrometer operating at 800 MHz for protons. The temperature dependence of the amide proton chemical shifts was determined by one-dimensional proton NMR experiments between 298 and 323 K on a 400 MHz Bruker Avance spectrometer. Cyclo(1,8)-CPRGGSVC peptide (5 mg) was dissolved in 900 μL phosphate buffer (pH 5.0, 20 mM) and 100 μL D_2O. Sodium 3-(trimethylsilyl)-1-propiosulfonic acid (DSS) was used as an internal reference for chemical shift calibration in ROESY and TOCSY experiments. Meanwhile, tetramethylsilane (TMS) was used for an internal standard in temperature dependence one-dimensional NMR experiments. The $3J_{NH\text{-}HC\alpha}$ scalar coupling constants were calculated from the backbone amide region of *F1* row of ROESY spectrum using Karplus equation:35

$$^{3}J_{NH-HC\alpha}=6.4\quad \cos^{2}\theta - 1.4\quad \cos\theta+1.9\quad ;\text{where}\quad \theta=|\varphi - 60^{\circ}|$$

Total correlation spectroscopy (TOCSY) and rotating-frame nuclear Overhauser enhancement spectroscopy (ROESY) experiments were carried out by presaturation of water during relaxation delay. Proton resonance assignments and spin system identification were made using a TOCSY spectrum with mixing time of 62 ms. ROE assignments and identification of sequential ROE connectivities were made using ROESY spectra with mixing times of 200 ms. The ROE cross-peak volumes were classified as strong, medium, and weak, and they were correlated to distances of $d_{N\alpha}(i, i)$, $d_{\alpha N}(i, i+1)$, and $d_{NN}(i, i+1)$ for which the upper limits were assigned as 2.4, 3.5, and 5.0 Å, respectively. Spectra visualization was performed using CARA (Institute of Molecular Biology and Biophysics, ETH Zurich, Switzrland) and MestReNova (Mestrelab Research S.L., Spain) softwares.

Molecular Dynamics Simulation

NMR-restraint molecular dynamics simulation was performed in MOE (Molecular Operation Environment) software (Chemical Computing Group, Quebec, Canada) using AMBER99 force field. The potential energy terms for AMBER99 force field is expressed in an equation below:36

$$E_{pot}=\sum_{\text{bonds}} K_r\left(r-r_{eq}\right)^2+\sum_{\text{angles}} K_\theta\left(\theta-\theta_{eq}\right)^2+\sum_{\text{dihedrals}} \frac{V_n}{2}\left[1+\cos\left(n\phi-\gamma\right)\right]+\sum_{i<j}\left[\frac{A_{ij}}{R_{ij}^{12}}-\frac{B_{ij}}{R_{ij}^{6}}+\frac{q_iq_j}{\varepsilon R_{ij}}\right]$$

where the total potential energy is the sum of bond stretching, angle bending, torsional angle, van der Waals, and electrostatic energies. ROE distance restraints were applied with upper limits of 2.8, 3.5, and 5.0 Å for strong, medium, and weak ROE peaks, respectively. A peptide bond (ω) dihedral angle restraint of 180 ± 10° was applied to keep all peptide bond as *trans*, except for Cys1-Pro2 peptide bond since the ROESY spectrum does not show the presence of $d_{\alpha\alpha}$ cross-peak between Cys1 and Pro2 as an indicator of *cis* X-Pro, and also the $d_{\alpha\delta}$ cross-peak between Cys1 and Pro2 as an indicator of *trans* XPro. A constant force of 10 kcal/mol.Å was applied. The starting structure was simulated at high temperature (600 K) and NPT (constant pressure) *in vacuo* using dielectric constants of 1 and 80 for 30 ps to relax the structure. The final structure was then soaked in a waterbox (with periodic system) and was simulated at 300 K for 1000 ps (NPT), time-step of 0.1 fs, temperature and pressure response of 0.1, respectively. Data were collected every 1 ps. The stability of the simulated molecule was monitored by observing the backbone RMSD values. The RMSD values of the last 500 ps of molecular dynamics simulation showed equilibrium condition with lesser fluctuation compared to the first 500 ps of molecular dynamics simulation. The trajectories from the last 500 ps of molecular dynamics simulation were taken for analysis. The following criteria were used to determine the best fit solution conformation of peptide: (i) the proton should have an interproton distance < 0.5 Å compared to the upper boundaries of distances from the ROE restraint; (ii) the conformation had φ angles within 30° of the calculated φ derived from $^3J_{\text{NH-HC}\alpha}$.25

Acknowledgments

This work is supported by the National Institutes of Health (R01-AI-063002). We also thank Nancy Harmony for proofreading the manuscript.

REFERENCES

1. Bromley SK, Burack WR, Johnson KG, Somersalo K, Sims TN, Sumen C, Davis MM, Shaw AS, Allen PM, Dustin ML. Annu Rev Immunol. 2001; 19:375–396. [PubMed: 11244041]
2. Davis DM, Dustin ML. Trends Immunol. 2004; 25:323–327. [PubMed: 15145322]
3. Grakoui A, Bromley SK, Sumen C, Davis MM, Shaw AS, Allen PM, Dustin ML. Science. 1999; 285:221–227. [PubMed: 10398592]
4. Bromley SK, Iaboni A, Davis SJ, Whitty A, Green JM, Shaw AS, Weiss A, Dustin ML. Nat Immunol. 2001; 2:1159–1166. [PubMed: 11713465]
5. Bromley SK, Dustin ML. Immunology. 2002; 106:289–298. [PubMed: 12100716]
6. Hogg N, Laschinger M, Giles K, McDowall A. J Cell Sci. 2003; 116:4695–4705. [PubMed: 14600256]
7. Blois S, Tometten M, Kandil J, Hagen E, Klapp BF, Margni RA, Arck PC. J Immunol. 2005; 174:1820–1829. [PubMed: 15699108]
8. Ragazzo JL, Ozaki ME, Karlsson L, Peterson PA, Webb SR. Proc Natl Acad Sci U S A. 2001; 98:241–246. [PubMed: 11120881]
9. Isobe M, Yagita H, Okumura K, Ihara A. Science. 1992; 255:1125–1127. [PubMed: 1347662]
10. Takazawa K, Hosoda Y, Bashuda H, Seino K, Yagita H, Tamatani T, Miyasaka M, Okumura K. Transplant Proc. 1996; 28:1980–1981. [PubMed: 8658967]
11. Gottlieb AB, Krueger JG, Wittkowski K, Dedrick R, Walicke PA, Garovoy M. Arch Dermatol. 2002; 138:591–600. [PubMed: 12020219]

12. Gordon KB, Papp KA, Hamilton TK, Walicke PA, Dummer W, Li N, Bresnahan BW, Menter A. JAMA. 2003; 290:3073–3080. [PubMed: 14679270]
13. Moriyama H, Yokono K, Amano K, Nagata M, Hasegawa Y, Okamoto N, Tsukamoto K, Miki M, Yoneda R, Yagi N, Tominaga Y, Kikutani H, Hioki K, Okumura K, Yagita H, Kasuga M. J Immunol. 1996; 157:3737–3743. [PubMed: 8871677]
14. Kavanaugh AF, Davis LS, Jain RI, Nichols LA, Norris SH, Lipsky PE. J Rheumatol. 1996; 23:1338–1344. [PubMed: 8856611]
15. Schulze-Koops H, Lipsky PE, Kavanaugh AF, Davis LS. J Immunol. 1995; 155:5029–5037. [PubMed: 7594511]
16. Weitz-Schmidt G, Welzenbach K, Brinkmann V, Kamata T, Kallen J, Bruns C, Cottens S, Takada Y, Hommel U. Nat Med. 2001; 7:687–692. [PubMed: 11385505]
17. Welzenbach K, Hommel U, Weitz-Schmidt G. J Biol Chem. 2002; 277:10590–10598. [PubMed: 11781316]
18. Anderson ME, Siahaan TJ. Pharm Res. 2003; 20:1523–1532. [PubMed: 14620502]
19. Yusuf-Makagiansar H, Anderson ME, Yakovleva TV, Murray JS, Siahaan TJ. Med Res Rev. 2002; 22:146–167. [PubMed: 11857637]
20. Gadek TR, Burdick DJ, McDowell RS, Stanley MS, Marsters JC Jr. Paris KJ, Oare DA, Reynolds ME, Ladner C, Zioncheck KA, Lee WP, Gribling P, Dennis MS, Skelton NJ, Tumas DB, Clark KR, Keating SM, Beresini MH, Tilley JW, Presta LG, Bodary SC. Science. 2002; 295:1086–1089. [PubMed: 11834839]
21. Jois DS, Pal D, Tibbetts SA, Chan MA, Benedict SH, Siahaan TJ. J Pept Res. 1997; 49:517–526. [PubMed: 9266479]
22. Anderson ME, Yakovleva T, Hu Y, Siahaan TJ. Bioorg Med Chem Lett. 2004; 14:1399–1402. [PubMed: 15006370]
23. Anderson ME, Tejo BA, Yakovleva T, Siahaan TJ. Chem Biol Drug Des. 2006; 68:20–28. [PubMed: 16923022]
24. Zimmerman T, Oyarzabal J, Sebastian ES, Majumdar S, Tejo BA, Siahaan TJ, Blanco FJ. Chem Biol Drug Des. 2007; 70:347–353. [PubMed: 17868072]
25. Gursoy RN, Jois DS, Siahaan TJ. J Pept Res. 1999; 53:422–431. [PubMed: 10406220]
26. Chou KC. Anal Biochem. 2000; 286:1–16. [PubMed: 11038267]
27. Iskandarsyah, Tejo BA, Tambunan US, Verkhivker G, Siahaan TJ. Chem Biol Drug Des. 2008; 72:27–33. [PubMed: 18554252]
28. Majumdar S, Kobayashi N, Krise JP, Siahaan TJ. Mol Pharm. 2007; 4:749–758. [PubMed: 17680719]
29. Wishart DS, Sykes BD, Richards FM. J Mol Biol. 1991; 222:311–333. [PubMed: 1960729]
30. Chou KC. Biopolymers. 1997; 42:837–853. [PubMed: 10904555]
31. Dyson HJ, Rance M, Houghten RA, Lerner RA, Wright PE. J Mol Biol. 1988; 201:161–200. [PubMed: 2843644]
32. Kessler H. Angew. Chem. Int. Ed. 1982; 21:512–523.
33. Shimaoka M, Xiao T, Liu JH, Yang Y, Dong Y, Jun CD, McCormack A, Zhang R, Joachimiak A, Takagi J, Wang JH, Springer TA. Cell. 2003; 112:99–111. [PubMed: 12526797]
34. Nam K, Maiorov V, Feuston B, Kearsley S. Proteins. 2006; 64:376–384. [PubMed: 16705652]
35. Pardi A, Billeter M, Wuthrich K. J Mol Biol. 1984; 180:741–751. [PubMed: 6084720]
36. Wang J, Cieplak P, Kollman PA. J Comp Chem. 2000; 21:1049–1074.

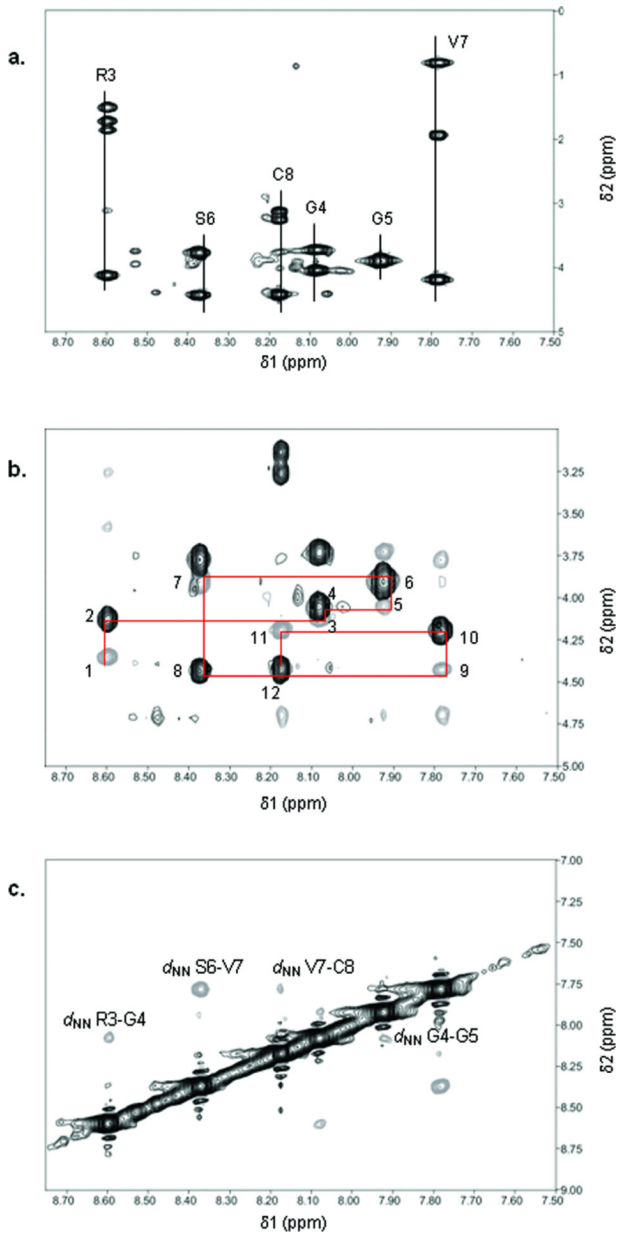

Figure 1.

(a) Fingerprint region of TOCSY spectrum of cyclo(1,8)-CPRGGSVC peptide. (b) NH-αH region of ROESY spectrum of cyclo(1,8)-CPRGGSVC peptide superimposed with the fingerprint region of TOCSY spectrum. The “backbone walk” of the ROESY/TOCSY spectrum used to determine the sequence of the peptide is shown by the sequential numbers. (c) NH-NH region of ROESY spectrum of cyclo(1,8)-CPRGGSVC peptide showing $d_{NN}(i, i+1)$ cross-peaks

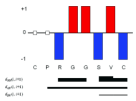

Figure 2.
Chemical shift indices (CSI, above the line) and summary of the inter-residue ROE effects among the backbone NH, αH, and βH (below). The CSI values were equal to 0 or were not calculated for amino acid residues with empty squares. The ROE intensities are reflected by the thickness of the lines.

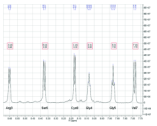

Figure 3.
One-dimensional NMR spectrum taken from *F2* row of ROESY spectrum of cyclo(1,8)-CPRGGSVC peptide. The value of $^{3}J_{\text{NH-HC}\alpha}$ was taken from amide proton peaks on this spectrum. The peak splitting is marked (d = doublet, t = triplet).

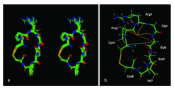

Figure 4.
Stereo-view of superimposed conformations of 10 structures taken from the last 500 ps molecular dynamics trajectories (a). The trajectory with lowest energy was taken for clarity (b). The hydrogen bonds between the backbone carbonyl group of Pro2 and amide protons of Gly4 and Gly5 are shown by yellow dashed lines. The distance between Cα of Pro2 and Cα of Gly5 is shown by an orange dashed line. The distance between Cα of Cys1 and Cα of Pro2 is shown by a turquoise dashed line.

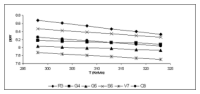

Figure 5.
Chemical shifts of amide protons of cyclo(1,8)-CPRGGSVC peptide at different temperatures. The slope of the curve ($\Delta\delta/\Delta T$) is the temperature coefficient of the amide proton.

Table 1

Chemical shift of amide proton resonance of cyclo(1,8)-CPRGGSVC peptide at 298 K

Residue	Chemical shift (ppm)				
	NH	CHα	CHβ	CHγ	CHδ
Cys1					
Pro2					
Arg3	8.60	4.12	1.87/1.73	1.51	3.10
Gly4	8.08	4.06/3.73			
Gly5	7.92	3.90			
Ser6	8.37	4.43	3.77		
Val7	7.78	4.18	1.93	0.81	
Cys8	8.17	4.43	3.26/3.13		

Table 2

Scalar coupling constant ($^3J_{NH\alpha H}$), calculated φ and simulated dihedral angles (φ and ψ) of cyclo(1,8)-CPRGGSVC peptide.

Residue	$^3J_{NH\alpha H}$ (Hz)	Calculated φ (deg.)	Structure (500–1000 ps)	
			φ (deg.)	ψ (deg.)
Cys1				−66.5
Pro2			−78.0	163.2
Arg3	6.65	48.5, 71.5, −79.46, −160.54	−88.6	−24.8
Gly4	5.48	30, 90, −70.28, −169.72	−72.1	15.2
Gly5	5.67	87.8, 242.2, −71.75, −168.25	171.7, −169.6	167.4, −174.7
Ser6	7.83	−89.25, −150.75	−148.2	99.7
Val7	8.61	−96.98, −143.02	−144.6	−56.5
Cys8	6.26	79.61, 40.39, −76.32, −163,68	−95.1	

Table 3

Interproton distances, energy, and geometry analyses of simulated cyclo(1,8)-CPRGGSVC peptide. The values of RMSD (root-mean square deviation) indicate how far the peptide NMR ensemble structures deviate from the lowest energy structure.

Residue	No. of ROE distance restraint	Violations (> 0.5 Å)
Cys1	0	n.d.
Pro2	0	n.d.
Arg3	11	0
Gly4	3	0
Gly5	2	0
Ser6	6	0
Val7	12	0
Cys8	3	0

Potential energy component	Average potential energy for NMR ensemble structures (kcal/mol)	S.D. (±)
Bond stretching	19.3	2.7
Angle bending	84.9	4.5
Improper torsion	6.4	1.5
Torsional angle	87.2	4.0
van der Waals	12.3	4.4
Electrostatic	−303.3	3.5
Total	−93.2	9.5
RMSD (backbone)	0.308	
RMSD (heavy atoms)	0.53	